J Polym Res (2011) 18:2469–2475
DOI 10.1007/s10965-011-9668-5

ORIGINAL PAPER

The effect of stretching on the morphological structures and mechanical properties of polypropylene and poly(ethylene-*co*-octene) blends

Lin Zhu · Xinhua Xu · Jing Sheng

Received: 25 March 2011 / Accepted: 11 July 2011 / Published online: 27 August 2011

Abstract Binary blends based on polypropylene and poly (ethylene-*co*-octene) were prepared in a co-rotating twin-screw extruder. A stretching process was carried out afterwards in the melt state at the extruder's exit to study the effect of stretching on morphological structures and mechanical properties. The morphological structures of the blends were investigated by scanning electron microscopy and small-angle X-ray scattering. The structure parameters, the correlation distance, the average chord lengths, and the Porod's index, obtained by the Debye-Bueche statistical theory of scattering were used to characterize the morphological structures. In addition, the relationship of mechanical properties with the structure parameters was also studied and some results were acquired.

Keywords Polypropylene (PP) · Poly(ethylene-*co*-octene) (PEOc) · Phase morphology · Mechanical properties

Introduction

Polymer blends were widely used because they provided better performance than homopolymers and they were more cost-efficient than synthesizing new polymers. So there had been substantial developments in both theory and application of polymer blends in the last few decades. In such two-phase or multiphase polymeric materials, there was a strong relation between morphological structure and physical properties [1].

Because of its outstanding properties such as high heat resistance, high mechanical strength, easy process ability and low price, polypropylene (PP) had become one of the most important commercial thermoplastics that was used in a myriad of products and processed in numerous ways. However, the plastic had two primary drawbacks, one was that it exhibited low impact toughness, especially at low temperatures and high deformation speeds, and the other was that it had poor melt strength. One of the most popular methods used to increase the impact strength and the melt strength was the addition of elastomers, which were blended with PP in the molten state. Ethylene–propylene rubber (EPR) [2, 3], ethylene-propylene-diene terpolymer (EPDM) [4, 5], styrene-ethylene butylenes-styrene triblock copolymer (SEBS) [6, 7] and, more recently, metallocenic ethylene-octene copolymer (EOC) [8–11] were the most commonly used elastomers to improve the mechanical properties of PP.

Different types of morphologies, such as dispersed, fibrillar, lamellar or co-continuous structures were known which could be formed by means of melt mixing [12]. The size and shape of the dispersed phase were the important factors that influenced the mechanical properties of polymer blends. Therefore, the control of phase morphology and structure of polymer blends was of vital importance for the tailoring of the final properties of the product [13, 14]. It was well known that during the melt processing of polymer blends, the final size, shape and distribution of the dispersed phase were determined by a variety of parameters such as the composition, viscosity ratio, shear rate/shear stress, elasticity ratio and interfacial tension among the

L. Zhu (✉)
School of Materials Science and Engineering, Jiangsu University,
301 Xuefu Road,
Zhenjiang 212013, China
e-mail: lzhu@ujs.edu.cn

X. Xu · J. Sheng
School of Materials Science and Engineering, Tianjin University,
92 Weijin Road,
Tianjin 300072, China

component polymers and processing conditions, such as time and temperature of mixing, rotation speed of rotor and type of mixing [14]. The deformation of polymer melt in polymer processing leaded to deformation of the particles of the dispersed phase, and different types of morphologies were formed [15].By careful selection of component polymers, their blend composition and processing conditions, one could obtain wide range of desirable properties in polymer blends.

The main objective of this paper was to investigate the effect of stretching on morphological structures and mechanical properties of PP/PEOc blends at different blend ratio. The relationship between mechanical properties (such as Young's modulus, tensile strength and yield strength) and the structure parameters (such as the non-uniform length ratio which was supposed to be oriented in one direction and the deformation factor) were studied in detail and some results were acquired.

Experimental

Materials

The basic polymers used in this study were a commercial grade isotactic polypropylene (PP1300) supplied by Beijing Yanshan Petrochemical Company, China, and a commercial grade poly(ethylene-co-octene) copolymer (PEOc, Engage 8150), a metallocene catalyzed copolymer with 25 wt% of comonomer provided by Dow Elastomers Company. Characteristics of the materials used were given in Table 1.

Blend preparation

The polymer blend with different compositions [PP/PEOc= 50/50, 60/40, 70/30, 80/20, 90/10, by volume concentration] was prepared using a 16 mm parallel, co-rotating twin-screw extruder (model Rheomex PTW24/40P).The screw length was 960 mm. The screw speed was 80 rpm and the mixing temperature was 200 °C. A stretching process was carried out afterwards in the melt state at the extruder's exit to study the effect of stretching on morphological structures and mechanical properties. The stretching speed and the extrusion speed were equal in all the sample preparation. The extrudates in sheet form were cooled in a water bath. The final extruded sheets were 30 mm in width and 0.5 mm in thickness. Prior to processing, PP and PEOc were dried under vacuum for 12 h at 80 °C and 50 °C, respectively.

Table 1 Characteristics of the polymers used in this work

Polymer	Density (kg/m^3)	MFI (g/10 min)[a]
PP	0.9	1.1
PEOc	0.9	0.5

[a] For PP, MFI was measured under 2.2 kg at 230 °C. For PEOc, MFI was measured under 2.2 kg at 190 °C

Morphological investigation

The phase morphology of the final extruded sheets was investigated using scanning electron microscope (Philips XL-30 ESEM). The sheets were fractured under liquid nitrogen for at least 10 min to make sure that the fracture was sufficiently brittle. The fractured surfaces parallel and perpendicular to the stretching direction were dipped in n-heptane at 60 °C for 15 min to extract the elastomer phase. Then the samples were dried for a period of 72 h and were coated with gold prior to SEM examination. Considering that the quality and resolution of SEM images were strongly affected by the thickness of the plated gold, the sputter time was strictly controlled to be identical for each sample. The microscope operating at 25 kV was used to observe the specimens, and several microscopy photographs were taken for each sample.

SAXS experiments

Square of 25 mm in sides and 0.5 mm in thickness were prepared by clipping the final extrudate. SAXS measurements were completed using the D/max-Ra x-ray diffraction (Rigaku, Japan). The experiments were conducted at the voltage of 40 kV, electric current of 1.50 mA, and the incident X-ray wavelength λ was 0.154 nm. A four-pinhole collimator system was used throughout the experiments. The scattering vector was denoted as h, $h=4\pi\sin\theta/\lambda$. The air scattering and absorption of the sample were corrected to obtain $I(h)$–h curves, where $I(h)$ was slit-smeared intensity.

Mechanical properties

The tensile properties were carried out using a Testometric M350-20KN tensile machine (Instron, Canton, MA) according to GB1040 at a crosshead speed of 50 mm/min and a testing temperature of 25±1 °C. The tensile specimen dimensions meet the requirement of GB1040 standard. The modulus was taken to be the initial slope of the stress–strain curve. An average of about ten samples was used for each property, and the reported values of the standard deviation were less than 10%.

Results and discussion

Phase morphology and structure studies of PP/PEOc blends

Figures 1 and 2 showed the SEM micrographs of the PP/PEOc blends in the parallel direction and the perpendicular

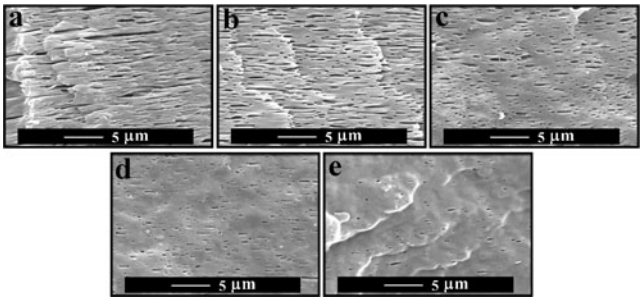

Fig. 1 SEM micrographs of the PP/PEOc blends at different concentrations (in the parallel direction). **a** 50/50, **b** 60/40, **c** 70/30, **d** 80/20, **e** 90/10

direction of the extrusion flow, respectively. From Fig. 1, it could be seen that the dispersed phase particles were almost spherical and uniform and no phase orientation or difference in shape of the dispersed domains was observed when the concentration of dispersed phase was low. However, the elliptical, rodlike and microfibril morphology appeared and they could also be oriented in the extrusion flow direction as the concentration increases. In addition, the dispersed phase dimension increase with increasing the concentration of the dispersed phase.

Drop-to-fibril transition in Newtonian fluids was previously studied by various investigators [16, 17]. They pointed out that the main factor for fibril formation was the viscosity ratio and a uniform thin-thread fibril was formed if the viscosity ratio was close to unity. In this work, every blend preparation was carried out under the same experimental conditions. So the viscosity ratio, the elasticity ratio and the interfacial tension remained invariable. The globular particles of the dispersed phases were mechanically stretched into dispersed phase rods and microfibrils without the presence of voids. This result could be due to the high compatibility in the melt state of PP and PEOc, because of their similar chemical structures and low interfacial tension. The dispersed phase rods and microfibrils were embedded into the continuous phase and the orientation of them increased with the increasing of the dispersed phase concentration. This was attributed to the

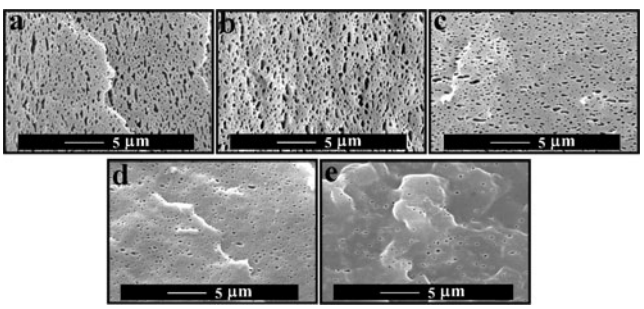

Fig. 2 SEM micrographs of the PP/PEOc blends at different concentrations (in the perpendicular direction). **a** 50/50, **b** 60/40, **c** 70/30, **d** 80/20, **e** 90/10

fact that it was more difficult to deform a small particle than a larger one, as predicted by Taylor' theory [16].

In the perpendicular direction of the extrusion flow (Fig. 2), the PEOc dispersed phase was dispersed in the PP matrix phase uniformly at low concentration of the dispersed phase. However, the dispersed phase size increased and the structure and shape of the particles became more and more complex as the concentration of the dispersed phase increased.

Although these micrographs showed a vivid phase structure and morphology, it was hard to quantitatively determine the variation of dispersed phase dimension and deformation degree of phase morphology just based on these micrographs. For this reason, the phase structure and morphology of PP/PEOc blends were further studied by small-angle X-ray scattering in the next section.

Small angle X-ray scattering studies of PP/PEOc blends

The phase morphology and structure of the PP/PEOc blends could be characterized by the SAXS using the structure parameter. The correlation distance (a_c) and average chord lengths (L) were obtained by Debye-Bueche scattering theory [18, 19]. For this purpose, a modification of the Debye–Bueche description of scattering from random heterogeneous media for spherical symmetrical systems was used [20, 21], which gave,

$$I_s(h)K\overline{\eta^2}\int_0^\infty \gamma(r)\frac{\sin(hr)}{hr}r^2dr \tag{1}$$

where K was a proportionality constant and $h=(4\pi/\lambda)\sin\theta$. $\overline{\eta}^2$ was the mean square fluctuation of the refractive index and η was the fluctuation in scattering power of the system, which for SAXS was equal to the deviation in polarization from its mean value at position r. $\gamma(r)$ was correlation function corresponding to fluctuation of medium and could be obtained by the inverse Fourier transform of $I(h)$. For systems with no clearly defined structure, $\gamma(r)$ often decreased monotonically with r and could be represented by an empirical equation, such as

$$\gamma(r) = \exp(-r/a_c) \tag{2}$$

where the parameter a_c was known as correlation distance and could be used to describe the size of the heterogeneity. For dilute discrete particles, a_c was related to the particle size. Thus, a_c was $(4/3)R$ for spheres. For more concentrated systems, a_c was not simply related to the size of the structural unit but depended upon both interparticle and intraparticle distances. It might be considered as an average wavelength of $\eta(x)$ fluctuations, whereas $\overline{\eta}^2$ was a mean-square amplitude.

If Eq. (2) was substituted into Eq. (1) one could obtain

$$I(h) = K'\overline{\eta^2}a_c^3\left(1 + h^2a_c^2\right)^{-2} \tag{3}$$

Upon rearrangement, this gave

$$[I(h)]^{-1/2} = \left(K'a_c^3\right)^{-1/2}\left(1 + h^2a_c^2\right) \tag{4}$$

Consequently, a plot of $I(h)^{-1/2}$ against h^2 should lead to a straight line having a ratio of slope to intercept of a_c^2, and the value of a_c was obtained.

An analysis might be made using the approach of Debye et al. [21] for a random dispersion of two phases of the volume fractions, φ_1 and φ_2, and a definite composition for which the ratio of the interphase surface area S to the volume V was related to the correlation distance by

$$S/V = 4\varphi_1\varphi_2/a_c \tag{5}$$

Kralky [22] and Stein [23] defined the average chord lengths L_1 and L_2. If lines were randomly drawn through the system in three dimensions, L_1 represented, for example, the mean length of the line segments through the regions of phase 1. These chord lengths were given by

$$L_1 = 4\varphi_1/(S/V) \tag{6}$$

$$L_2 = 4\varphi_2/(S/V) \tag{7}$$

from which it followed that

$$L_1 = a_c/\varphi_2 \tag{8}$$

$$L_2 = a_c/\varphi_1 \tag{9}$$

Here, average chord lengths could be calculated using a_c by Eqs. (8) and (9).

Figure 3 showed the variations of correlation distance a_c and average chord lengths L_{PEOc} of dispersed phase PEOc as the function of concentration of PEOc. Obviously, the size of dispersed phase particles was small when the concentration of the dispersed phase PEOc was low and the size of the dispersed phase domains increased when the content of the dispersed phase rose. But, the increment was not very distinct when the volume fraction of PEOc was lower than 30%. This phenomenon indicated that the increase in PEOc concentration first raised the number of domains but not their size. Only when the volume fraction of PEOc was higher than 30%, the number of domains approached to saturation and the size of these domains increased greatly. In addition, it could be seen that the value of a_c had a similar variation with average chord lengths L_{PEOc}, and the a_c just increased more slowly than the average chord lengths of PEOc.

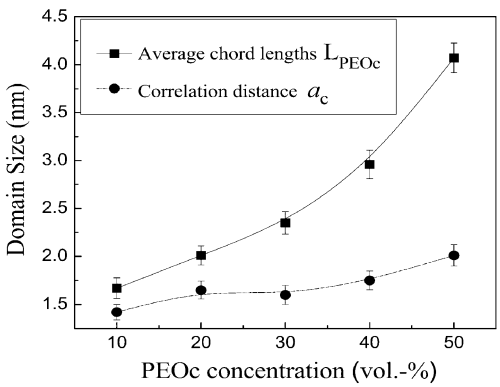

Fig. 3 Relation of correlation distance a_c and average chord lengths L_{PEOc} with composition of PP/PEOc blends

The variation of L_{PP} and L_{PEOc} with concentration of PEOc in the PP/PEOc blends was shown in Fig. 4. The value of the variation for L_{PEOc} increased slowly with the PEOc concentration increasing. However, the value of the variation for L_{PP} increased quickly with the decreasing of PEOc concentration, and the variation of the value of L_{PP} was larger. This result indicated that the PP phase was a continuous phase at a larger region of compositions in the blends.

To further characterize the structure of the dispersed phase in PP/PEOc blends, the scattering spectra were analyzed using Guinier and Fournet [24] and the Porod [25] analyses. The Porod region was examined to evaluate approximately the structure and shape of the dispersed phase PEOc particles. Porod derived that

$$\ln I(h) \sim -\alpha \ln(h) \tag{10}$$

$\ln I(h)$ as a function of $\ln(h)$ should be equal to $-\alpha$ at α large h value. The Porod index α was obtained from this equation. If α was equal to (or approaches) 1, the particles were rodlike in shape. When α was equal to 2, these

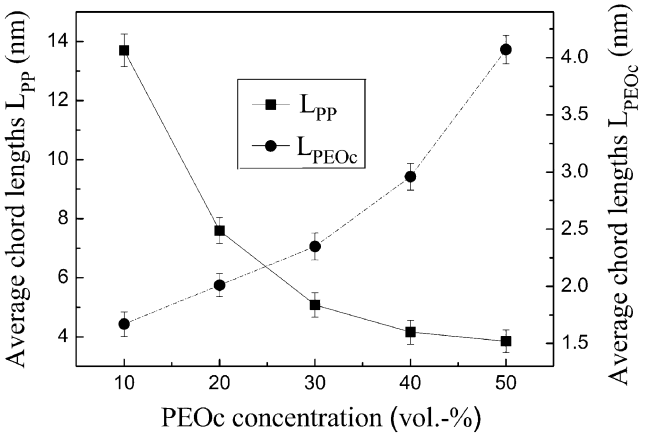

Fig. 4 Relation of average chord lengths L_{PP} and L_{PEOc} with composition of PP/PEOc blends

particles were flat particles. In the case of α equal to 4, these particles were spherical in shape and had a smooth surface. The value of α was shown in Table 2.

The results indicated that the value of α was between 2 and 3 except for the composition of 50/50 which was smaller than 2. In addition, the value of α decreased as the PEOc concentration increased. The dispersed phase PEOc particles deformed and oriented during the extrusion process and subsequent stretching process. Obviously, the shape of the dispersed phase was not spherical or flat. The shape of the dispersed phases PEOc particles was random (near ellipsoidal), and it was more likely to be ellipsoidal morphology as the PEOc concentration increased. The shape became rodlike at the concentration of 40/60 and 50/50. This result was the same as that of the SEM image.

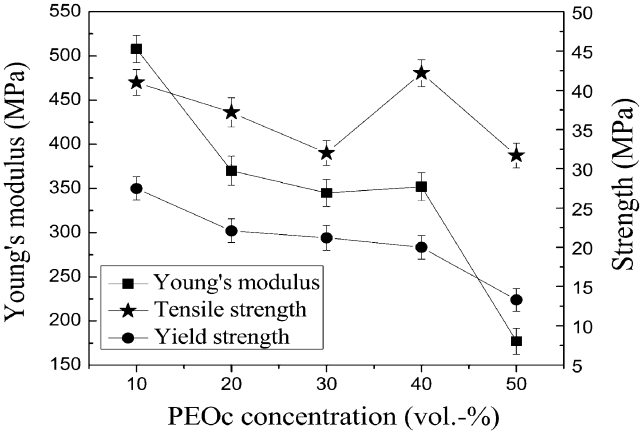

Fig. 5 The mechanical properties of PP/PEOc blends as a function of the volume fraction of PEOc

Relationship of mechanical property with morphological structure

The Young's modulus, yield strength and tensile strength values of PP/PEOc blends, for tests carried out at room temperature, were reported in Fig. 5 as a function of the volume fraction of PEOc. As shown in Fig. 5, the blends' modulus decreased with increasing PEOc concentration as was to be expected. The reason for the modulus's decrease with increasing of PEOc content in the PP/PEOc blend could be attributed to the fact that, since PEOc particles had very low shear modulus compared to PP, there was little or no stress transfer from matrix to elastomer particles. Therefore, the dispersed phase PEOc particles had almost the same effects as micro-voids on these mechanical properties. As well known, the yield strength and tensile strength measured at large deformations were much more dependent upon interfacial adhesion with respect to Young's modulus, measured at very small deformations. Similarly, two values also decreased as the PEOc content increased. It had been reported in the literature [26] that this behavior was related to the immiscibility of the components and consequent formation of a bi-phase structure.

Furthermore, these values decreased in a nonlinear manner as the volume fraction of PEOc increased, which meant the mechanical properties were not only related to the blend composition but also the morphological structure (such as the phase dimension, the phase distribution and the interfacial energy, etc.). However, when compared to the study of phase behavior, there had been only limited studies available on the mechanical properties of polypropylene and blends of different copolymers samples, which systematically dealt with the correlation between morphological structure and the macroscopic mechanical properties. Therefore, the relation between the mechanical properties and the corresponding structure parameter would be discussed as follows.

To obtain further information on the phase structure and morphology of PP/PEOc blends, a parameter called the deformation factor ξ (that was apparent uniform ratio of the dispersed phase particles in the orientation direction) was brought in to describe the extent of fibrous shape of the dispersed phase in the extrusion flow direction [27, 28]. The bigger the parameter, the closer to fibrous shapes the dispersed phase particles. The deformation factors of dispersed phase at different concentrations were listed in Table 2.

Figure 6 illustrated the variation of the Young's modulus, tensile strength, and yield strength with the deformation factor ξ. The results indicated that these mechanical property parameters first increased and then decreased with the increasing of deformation factor. The Young's modulus and yield strength had no obvious variation as the deformation factor increased when the deformation of the dispersed phase was small, while the tensile strength tended to increase. When the deformation factor of the dispersed

Table 2 The parameters for PP/PEOc blends at different concentrations

Parameters	Concentrations (vol/vol)				
	50/50	60/40	70/30	80/20	90/10
Porod's index	1.8	2.2	2.5	2.3	2.6
The deformation factor	30.1	3.9	7.3	4.2	22.1
The non-uniform length ratio	0.04	0.06	0.07	0.09	0.6

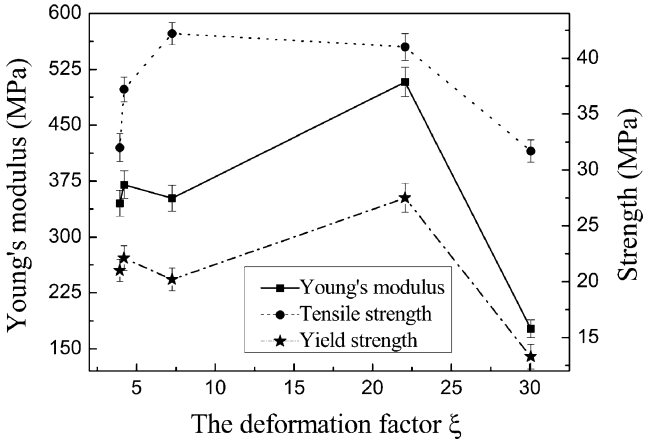

Fig. 6 Relation of mechanical properties with the deformation factor ξ

phase was 23, the Young's modulus, tensile strength, and yield strength all basically reached maximum, then they decreased as the deformation factor further increased. Therefore, the phase morphology and structure of the blends had great influence on the mechanical properties.

It was well known that crazing was a typical kind of nonlinear deformation in polymer blends. Great energy must be consumed during crazing initiation, growth and fracture, thus crazing was very important for polymer toughening design. The craze growth and fracture laws concerning with the craze architecture were the core of craze toughening mechanism. When the deformation of the dispersed phase was small, the subtle variation of phase morphology and structure had little effect on the Young's modulus and yield strength. But, when the sample was further stretched over the yield point, especially the stress hardening of the sample started to occur, the subtle variation of phase morphology and structure exerted an important influence on the mechanical properties, so tensile strength increased more than the Young's modulus and yield strength. As the deformation factor increased, the growth of crazing induced by the dispersed phase PEOc particles was limited and tended to be terminated by other PEOc particles. So the mechanical properties of PP/PEOc blends reduced. When the deformation factor ξ was in the appropriate range (it was about 23 in this system), the growth space of the crazing induced by the dispersed phase increased and would not be terminated so quickly by other PEOc particles. So the mechanical property parameters reached maximum when the deformation factor ξ was 23.

It was well known that the force was bearing mainly by the PP phase during the tensile test, the effect of the PP phase should be considered. So, another parameter called the non-uniform length ratio *LR* was brought in to study the morphological structure. It could be obtained from the SEM images. The uniformity degree of phase distribution could be described by the parameter *LR* from its physical significance. It was significant no matter what the shape of the dispersed phase PEOc was.

Figure 7 illustrated the variation of the Young's modulus, tensile strength and yield strength with the non-uniform length ratio *LR*. It could be seen that these mechanical property parameters decreased with the increase of *LR*. The Young's modulus and yield strength decreased in the exponential formula with *LR*, while tensile strength decreased in the linear formula.

Conclusions

The effect of stretching on morphological structures and mechanical properties was discussed in order to relate the macroscopic properties of PP/PEOc blends with morphological structures. Based on SEM observations, the morphological structures of the blends at different composition obtained from the fracture surfaces in the parallel direction and the perpendicular direction of the extrusion flow revealed a non-uniform and unstable morphology owing to the stretching process. The structure parameters of SAXS in the blends, such as the correlation distance (a_c) and average chord lengths (L), were calculated to characterize the phase dimension. The size of dispersed phase particles was small when the concentration of the dispersed phase was low and the size of the dispersed phase domains increased when the content of the dispersed phase rose. The shape of the dispersed phase was shown by Porod's index α, and its value was between 2 and 3 except for the composition of 50/50 which was smaller than 2. In addition, the value of α decreased as the PEOc concentration increased. The results indicated that the dispersed phase PEOc particles deformed and oriented during the extrusion process and subsequent stretching process. In addition, the relationship of mechanical properties with the

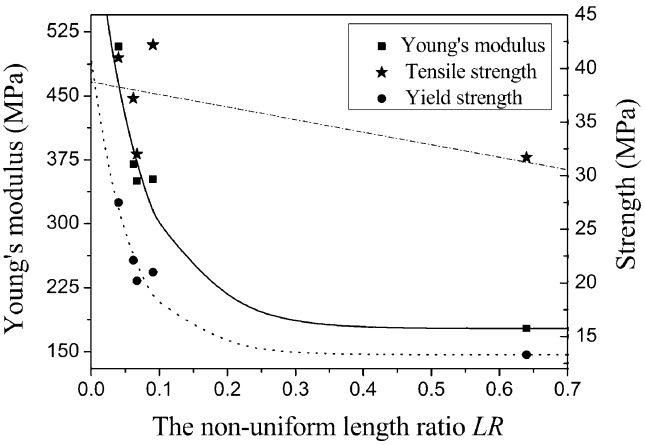

Fig. 7 Relation of mechanical properties with the non-uniform length ratio *LR*

structure parameters, such as the deformation factor and the non-uniform length ratio, was also studied and the results showed that the mechanical properties were not only related to the blend composition but also the phase structure.

Acknowledgements The authors gratefully acknowledge the financial support of National Natural Science Foundation of China (No. 20490220), China Postdoctoral Science Foundation (No. 20110491350), and the Senior Intellectuals Fund of Jiangsu University (No. 10JDG135).

References

1. Paul DR, Newman S (1978) Polymer blends, vols. 1 and 2. Academic, New York
2. Naiki M, Matsumura T, Matsuda M (2002) J Appl Polym Sci 83:46–56
3. Mae H (2008) Mater Sci Eng A 496:455–463
4. Chen Y, Li H (2004) Polym Eng Sci 44:1509–1513
5. Feng WL, Isayev AI (2004) Polymer 45:1207–1216
6. Ao YH, Tang K, Xu N, Yang HD, Zhang HX (2007) Polym Bull 59:279–288
7. Mader D, Bruch M, Maier RD, Stricker F, Mulhaupt R (1999) Macromolecules 32:1252–1259
8. McNally T, McShane P, Nally GM, Murphy WR, Cook M, Miller A (2002) Polymer 43:3785–3793
9. Zhu L, Xu XH, Wang FJ, Song N, Sheng J (2008) Mater Sci Eng A 494:449–455
10. Zhu L, Song N, Xu XH (2009) Macromol Mater Eng 294:516–524
11. Yao YH, Dong X, Zhang CG, Zou FS, Han CC (2010) Polymer 51:3225–3229
12. Macosko CW (2000) Macromol Symp 149:171–184
13. Martuscelli E, Palumbo R, Kryszewski M (1979) Polymer blends: processing, morphology and properties. Plenum Press, New York
14. Thomas S, Groeninckx G (1999) J Appl Polym Sci 71:1405–1429
15. Sundararaj U, Macosko CW (1995) Macromolecules 28:2647–2657
16. Taylor GI (1934) Proc Roy Soc Lond A 146:501–523
17. Torza S, Cox RG, Mason SG (1972) J Colloid Interface Sci 38:395–411
18. Debye P, Bueche AN (1949) J Appl Phys 20:518–525
19. Khambatta FB, Warner K, Russell T, Stein RS (1976) J Polym Sci Polym Phys Ed 14:1391–1424
20. Porod G (1952) Kolloid Z 125:51–57
21. Debye P, Anderson HR, Brumberger H (1957) J Appl Phys 28:679–683
22. Kralky O (1966) Pure Appl Chem 12:483–523
23. Stein F (1955) Trans Faraday Soc 51:430–441
24. Guinier A, Fournet G (1955) Small Angle Scattering of X-rays. Chapman and Hall, London, p 340
25. Porod G (1982) In: Glatter O, Krtky O (eds) Small Angle X-ray Scattering. Academic, New York, p 34
26. van der Wal A, Mulder JJ, Oderkerk J, Gaymans RJ (1998) Polymer 39:6781–6787
27. Wan ZM, Xie ZM, Sheng J (2003) Acta Materiae Compositae Sinica 20:100–105
28. Willemse RC, Speijer A, Langeraar AE, Posthuma de Boer A (1999) Polymer 40:6645–6650